New Constraints on the Early Expansion History of the Universe

Alireza Hojjati,[1] Eric V. Linder,[1,2] and Johan Samsing[3]

[1]*Institute for the Early Universe WCU, Ewha Womans University, Seoul 120-750, Korea*
[2]*Berkeley Center for Cosmological Physics and Berkeley Lab, University of California, Berkeley, California 94720, USA*
[3]*Dark Cosmology Centre, Niels Bohr Institute, University of Copenhagen, Juliane Maries Vej 30, 2100 Copenhagen, Denmark*

(Received 22 April 2013; published 24 July 2013)

Cosmic microwave background measurements have pushed to higher resolution, lower noise, and more sky coverage. These data enable a unique test of the early Universe's expansion rate and constituents such as effective number of relativistic degrees of freedom and dark energy. Using the most recent data from Planck and WMAP9, we constrain the expansion history in a model-independent manner from today back to redshift $z = 10^5$. The Hubble parameter is mapped to a few percent precision, limiting early dark energy and extra relativistic degrees of freedom within a model-independent approach to 2%–16% and 0.71 equivalent neutrino species, respectively (95% C.L.). Within dark radiation, barotropic ether, and Doran-Robbers models, the early dark energy constraints are 3.3%, 1.9%, and 1.2%, respectively.

DOI: 10.1103/PhysRevLett.111.041301 PACS numbers: 98.80.Es, 95.36.+x, 98.70.Vc

Except for the last e fold of cosmic expansion, our knowledge of the state of the Universe arises directly only through measurements of the cosmic microwave background (CMB) radiation or indirectly (as in models of its influence on growth of large scale structure). Recent CMB data [1,2] provide a clear window on an additional 10 e folds of history (back to redshift $z = 10^5$), a vast improvement in mapping the Universe.

The expansion rate, or Hubble parameter, is a fundamental characterization of our Universe and includes information on its matter and energy components, their evolution, and the overall curvature of spacetime. Moreover, the CMB encodes linear perturbations in the photons and the gravitational potentials they experience, providing sensitivity to the microphysics of components, e.g., their sound speed.

These observations lead to constraints on quantities such as early dark energy and extra neutrino species or other relativistic degrees of freedom. However, most analyses assume a specific model for these deviations, enabling stringent but model-dependent constraints. In this Letter, our approach is to map the cosmic state and history in as model-independent fashion as practical, guided by the data. We utilize the results of the principal component analysis of Ref. [3] to define localized bins of Hubble parameter in log scale factor that are most sensitive to the data and then carry out a Markov chain Monte Carlo (MCMC) analysis to constrain them. Finally, we discuss the implications for dark energy, relativistic degrees of freedom, and spacetime curvature. For data, we use the most recent CMB results from the Planck satellite [1] and the WMAP satellite [2].

Cosmic history mapping.—For robust, model-independent results, we adopt a combination of principal component analysis (PCA) and binning. This avoids assuming a specific functional form for the Hubble parameter or dark components and allows the data to inform where the greatest sensitivity lies. Such PCA on the Hubble parameter for projected mock CMB data was used in Ref. [3] to predict the strength of constraints at various epochs of cosmic history.

This identification of the key epochs where physical conditions most affect the observations enables an informed choice of bins in log scale factor to use in a MCMC fit. Bins have several advantages over the raw PCA: (1) they are localized and can be clearly interpreted physically—the Hubble parameter during a specific epoch, (2) they avoid negative oscillations that can cause unphysical results [while the sum of all principal components (PCs) will give a positive, physical Hubble parameter squared, this is not guaranteed for a subset], and (3) they are well defined, not changing when new data are added.

The Hubble parameter, or logarithmic derivative of the scale factor, $H = d\ln a/dt$, is then written as

$$H^2(a) = \frac{8\pi G}{3}[\rho_m(a) + \rho_r(a) + \rho_\Lambda][1 + \delta(a)], \quad (1)$$

where δ accounts for any variation from ΛCDM (cosmological constant plus cold dark matter plus standard radiation) expansion history, and ρ_m is the matter density, ρ_r the radiation density, and ρ_Λ the cosmological constant density. The bins in the deviation $\delta(a)$ are slightly smoothed for numerical tractability, with

$$\delta = \sum_i \delta_i \left[\frac{1}{1 + e^{(\ln a - \ln a_{i+1})/\tau}} - \frac{1}{1 + e^{(\ln a - \ln a_i)/\tau}}\right]. \quad (2)$$

Within bin i, $\delta = \delta_i$, and far from any bin $\delta = 0$. A smoothing length $\tau = 0.08$ was adopted after numerical convergence tests. (A similar binned approach was used in Refs. [4,5] to bound early cosmic acceleration.)

We modify CAMB [6] to solve the Boltzmann equations for the photon perturbations in this cosmology. The dark

energy density contributed by the deviations δ and the cosmological constant term (which becomes negligible at high redshift) has an effective equation of state

$$1 + w = \frac{Q\delta}{1 + \delta(1 + Q)}(1 + w_{\rm bg}) - \frac{1}{3}\frac{1 + Q}{1 + \delta(1 + Q)}\frac{d\delta}{d\ln a}, \quad (3)$$

where $Q = (\rho_m + \rho_r)/\rho_\Lambda$ and $w_{\rm bg}$ is the background equation of state of the combined matter and radiation (e.g., $1/3$ during radiation domination, transitioning to 0 during matter domination). Thus, w and $w' = dw/d\ln a$, entering into the Boltzmann equations, are defined fully by Eq. (2) for δ. We choose the associated sound speed to be the speed of light, as in quintessence dark energy, but explore variations of this later.

Guided by the PCA of Ref. [3], where the first few PCs show the greatest sensitivity in $\log a \in [-4, -2.8]$, we choose bins δ_{1-5} in the logarithmic scale factor $\log a = [-5, -4]$, $[-4, -3.6]$, $[-3.6, -3.2]$, $[-3.2, -2.8]$, $[-2.8, 0]$, so the finest binning is near CMB recombination at $a \approx 10^{-3}$. (Future CMB data could change the PCs, but we could keep the same bins, or not.) The cosmological parameters we fit for are the six standard ones: physical baryon density $\Omega_b h^2$, physical cold dark matter density $\Omega_c h^2$, acoustic peak angular scale θ, primordial scalar perturbation index n_s, primordial scalar amplitude $\ln(10^{10} A_s)$, and optical depth τ, plus the five new deviation parameters δ_{1-5}. Additional astrophysical parameters enter from the data, as discussed next.

Constraints.—To constrain the cosmology with the data, we use MCMC analysis, modifying COSMOMC [7]. The likelihood involves the temperature power spectrum from the two satellite experiments, and the E-mode polarization and TE cross spectrum from WMAP. (The first Planck likelihood release does not include polarization or the high multipole likelihoods from Atacama Cosmology Telescope [8] or South Pole Telescope [9]; in the future, such data should become available.) Astrophysical nuisance parameters characterizing foregrounds (see Ref. [1]) are marginalized over.

Figure 1 shows the constraints on the standard cosmological parameters, in the ΛCDM case (fixing $\delta_i = 0$) and when allowing variations in the expansion history (fitting for the δ_i). Here, the Hubble constant H_0 replaces the θ parameter and we omit showing τ. Including the fitting for expansion history deviations induces roughly a factor of 2 larger marginalized estimation uncertainties for most of the standard cosmology parameters, and significantly shifts the cold dark matter density value. This is due to the deviations in the Hubble parameter having similar effects on the expansion near recombination to those in matter, so δ takes the place of some of ρ_m. We discuss this degeneracy further later. The best fit for the ΛCDM case remains within the 68% confidence contour when allowing expansion deviations.

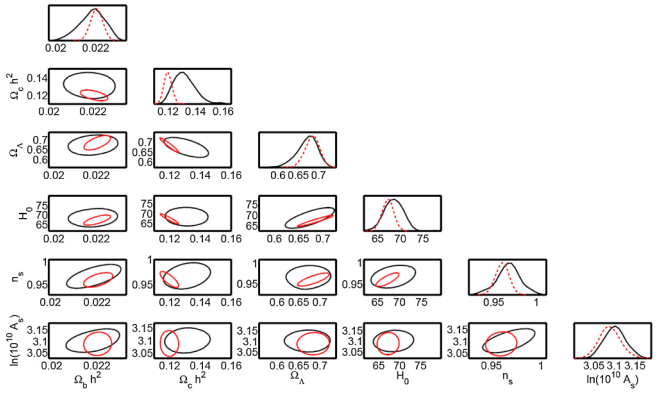

FIG. 1 (color online). Joint 68% confidence contours on the standard cosmological parameters are shown when allowing for expansion history deviations from ΛCDM (black) and fixing to ΛCDM (smaller contours or dashed curves). Plots on the diagonal give the 1D marginalized probability distributions.

Figure 2 shows the constraints on the expansion history deviations. Note that to ensure positive energy density (and Hubble parameter squared), we restrict $\delta \geq 0$, i.e., equal or more early energy density than in the ΛCDM case (which has $\Omega_\Lambda \approx 10^{-9}$ at $a = 10^{-3}$; allowing the limiting non-negative energy density $\delta \approx -10^{-9}$ would have negligible impact on the distributions). Note that these binned deviations do not have appreciable covariances with each other, with the correlation coefficients under 0.26 except for δ_2–δ_3 at 0.49. This is a useful feature, adding near independence to localization, making their interpretation transparent, and is a result of the careful choice of bins based on the PCA of Ref. [3].

Table I gives the 95% confidence upper limits on each expansion deviation parameter, showing that recent CMB data provide 2%–16% constraints on the expansion history back to $z = 10^5$. The earliest bin, of δ_1, is reasonably

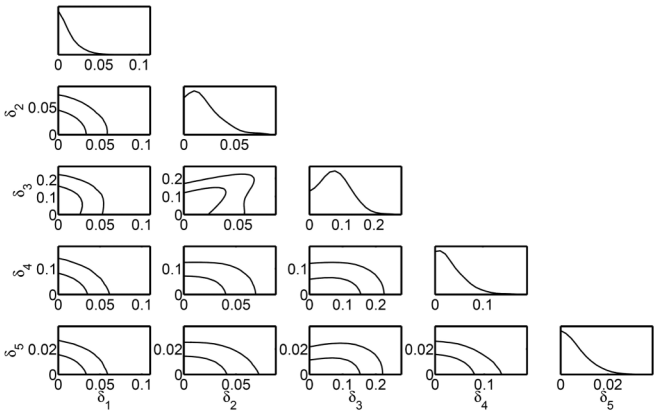

FIG. 2. Joint 68% and 95% confidence contours on the expansion deviation parameters are shown. Plots on the diagonal give the 1D marginalized probability distributions.

TABLE I. 95% confidence upper bounds are given for the expansion history deviations δ, listed by the bin number and midpoint of the log$a$ bins, for cases with different sound speeds.

Case	$\delta_1(10^{-4.5})$	$\delta_2(10^{-3.8})$	$\delta_3(10^{-3.4})$	$\delta_4(10^{-3.0})$	$\delta_5(10^{-1.4})$
$c_s^2 = 1$	0.036	0.050	0.160	0.095	0.018
$c_s^2 = 1/3$	0.053	0.054	0.067	0.038	0.013
$c_s^2 = 0$	0.060	0.069	0.109	0.184	0.223

constrained, despite being well before recombination, and should improve further when adding high resolution (high multipole l) measurements. The second bin has equivalent constraints when taking into account its narrowness. Around recombination, however, δ_3 and δ_4 have looser bounds because all the standard cosmological parameters also enter strongly at this epoch, and so the increased covariance dilutes their estimation. They have the two highest correlation coefficients, of 0.89 between δ_3 and $\Omega_c h^2$ and -0.76 between δ_4 and $\Omega_b h^2$. Finally, the late, broad bin of δ_5 has strong constraints. These behaviors are all consistent with the pre-Planck, Fisher matrix predictions of Ref. [3] (see their Fig. 4). Adding late time data or priors (which we avoid; see the concluding section) can shrink some uncertainties by up to 60%.

The expansion history does not completely define the system of Boltzmann equations: the effective dark component can have internal degrees of freedom such as sound speed c_s that determine the behavior of its perturbations and hence the gravitational clustering of the photons [10]. Therefore, we also show in Table I the constraints when this sound speed is equal to that of a relativistic species ($c_s^2 = 1/3$) or is much smaller than the speed of light, cold dark energy with $c_s = 0$. The $c_s = 0$ case has looser bounds, due to the additional influence on the photon clustering with the strengthened gravitational potentials and to covariance with matter parameters during matter domination. For the $c_s^2 = 1/3$ case, where the extra expansion rate corresponds to extra relativistic degrees of freedom, the constraints are weaker during radiation domination. This is a combination of the expansion deviation acting just like the photons and a slight preference of the data for additional radiation energy density, in accord with previous hints that the number of effective neutrino species $N_{\rm eff}$ might be greater than the standard model value of 3.046. Indeed, the mean value of $\delta_2 = 0.026$ in this case corresponds to $\Delta N_{\rm eff} = 0.31$, in good agreement with the Planck values of $N_{\rm eff} = 3.39$. Recall that $\Delta N_{\rm eff}$ denotes the equivalent number of relativistic neutrino species corresponding to the extra energy density. Since δ_2 is not in the fully radiation dominated era, we must translate it to the constant early dark energy density using Eq. (25) of Ref. [3] and then to the asymptotic relativistic $\Delta N_{\rm eff}$ using Eq. (6) of Ref. [11].

In all other parts of the Letter, we keep $c_s = 1$.

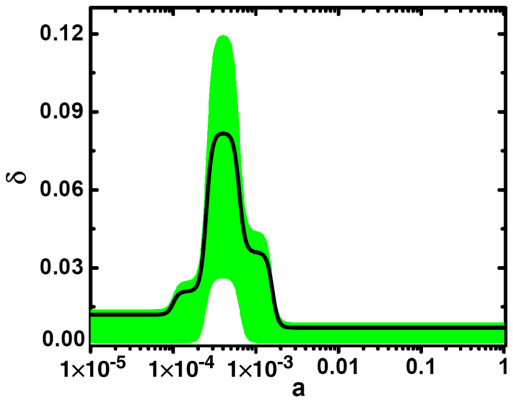

FIG. 3 (color online). Reconstruction of the expansion history deviations $\delta(a)$ from ΛCDM is shown, with the mean value (solid line) and 68% uncertainty band (shaded area).

Figure 3 shows the mean value and 68% uncertainty band of the expansion deviations $\delta(a)$ given by the Monte Carlo reconstruction using the recent CMB data. This figure represents the best current model-independent knowledge of the early expansion history of our Universe. Setting all $\delta_i = 0$, i.e., ΛCDM, is consistent with these results at the 95% confidence level. The mean value does show a very slight preference for a faster expansion rate, as in early dark energy or extra relativistic degrees of freedom, before recombination.

Physical implications.—This analysis has been model independent, allowing individual epochs to float freely without assuming a functional form. If we do assume a specific model, then constraints will in general be tighter, with each epoch having leverage on others through the restricted form.

Three distinct families of early dark energy might be considered: where the early dark energy density rises, falls, or stays constant across CMB recombination. These were investigated in Ref. [3] in terms of the (somewhat motivated) models of barotropic ether, dark radiation, and Doran-Robbers [12] forms, respectively (see Ref. [3] for more detailed discussion). We compute the constraints on the fraction Ω_e of critical density contributed by early dark energy (approximately equivalent to δ) within each of these models (not using the δ_i bins), giving the results in Table II. (Note that Planck finds $\Omega_e < 0.009$ at 95% C.L. for the Doran-Robbers model when also including high multipole data [13].)

TABLE II. The 95% confidence level uncertainties are presented for three early dark energy models. For small values, $\Omega_e \approx \delta$. The Doran-Robbers model has an additional parameter w_0; we find $w_0 = -1.49^{+0.69}_{-0.57}$ (95% C.L.).

	Ether	Dark radiation	Doran-Robbers
Ω_e	0.019	0.033	0.012

Two aspects of the models impact their detectability: the presence of the expansion history deviation at a sensitive epoch and its persistence over time, and its clustering behavior. The common Doran-Robbers form has the tightest bounds (despite the extra parameter), due to its persistence pre- and postrecombination and its distinction from matter clustering since it has $c_s^2 = 1$. The ether model only begins to deviate around recombination and has $c_s^2 = 0$, so there is more covariance with the dark matter component. Dark radiation has influence only before recombination, and its $c_s^2 = 1/3$ makes it more covariant with the photons (and neutrinos). A key conclusion is that early dark energy could in fact be more prevalent than apparent from bounds in the literature on the Doran-Robbers model.

Since dark radiation density at early times scales like radiation, it acts like the addition of relativistic degrees of freedom. Taking into account the definition of extra degrees in terms of the number of effective neutrino species $N_{\rm eff}$, the constraint on Ω_e within the dark radiation model translates to [11]

$$\Delta N_{\rm eff}(a \ll a_{\rm eq}) = 7.44\Omega_e/(1-\Omega_e). \quad (4)$$

Thus, $\Omega_e < 0.033$ for the dark radiation model becomes $\Delta N_{\rm eff} < 0.25$ at 95% C.L. This puts a tighter global bound on $\Delta N_{\rm eff}$ compared to our model-independent value from δ_2 before recombination ($\Delta N_{\rm eff} < 0.71$ at 95% C.L., where again we have to account for δ_2 not being in the fully radiation dominated era).

Another implication of the expansion history is its relation to the spacetime itself. The Ricci scalar curvature is the central quantity in the Einstein-Hilbert action for general relativity and plays a key role as well in extensions to gravity such as $f(R)$ theories. The curvature history of the Universe has been explored from a theoretical perspective recently by Ref. [14]. Since

$$R = 3H^2\left[1 - 3w_{\rm bg}\frac{H_{\rm fid}^2}{H^2} - 3w\frac{\delta H^2}{H^2}\right] \quad (5)$$

$$= 3H_{\rm fid}^2[1 - 3w_{\rm bg} + \delta(1-3w)], \quad (6)$$

observational constraints on δ [and hence w through Eq. (3)] can be used to cast light on the curvature history.

Conclusions.—We have used the recent advances in CMB data to constrain the fundamental quantity of the expansion history of our Universe. The results from the model-independent analysis bound deviations from ΛCDM at 2%–16% (95% C.L.), depending on the epoch. This constrains any deviations, whether due to, e.g., some form of dark energy or a nonstandard number of relativistic degrees of freedom. It also relates directly to the Ricci spacetime curvature.

Adding late time data that help to constrain H_0 or Ω_m, say, would help break the degeneracy around recombination that led to the loosest, 16% upper bound on deviations. However, proper treatment of this would require many low redshift bins to reflect the density of the data, while our focus here is on the early expansion history.

We regard the model independence of the analysis as a signal virtue; however, we can also compare the bounds for specific early dark energy models. For the barotropic ether, dark radiation, and Doran-Robbers models, we derive 95% C.L. limits of less than 0.019, 0.033, and 0.012 in early dark energy density Ω_e, respectively. We emphasize that bounds appear tightest when assuming the conventional Doran-Robbers form, and so early dark energy should be not be thought to be ruled out based purely on constraining this model. In terms of extra effective neutrino species, the model-independent results imply $\Delta N_{\rm eff} < 0.71$ at 95% C.L.

Future CMB data, such as the release of polarization data from Planck, ACTpol [15], PolarBear [16], and SPTpol [17] experiments will enhance our knowledge of the history back to $z \approx 10^5$. Exploring the even earlier universe will require neutrino, dark matter, or gravitational wave astronomy. Late time probes will continue to map the last e fold of cosmic expansion in greater detail. Over just a few years, cosmological observations have taken us from order unity uncertainty (with $\gtrsim 10\%$ in narrow epochs around recombination and today) to a few percent level knowledge over more than 10 e folds of cosmic history.

We thank Stephen Appleby, Scott Daniel, and Tristan Smith for helpful discussions. A. H. acknowledges the Berkeley Center for Cosmological Physics for hospitality. This work has been supported by WCU Korea Grant No. R32-2009-000-10130-0 and the Director, Office of Science, Office of High Energy Physics, of the U.S. Department of Energy under Contract No. DE-AC02-05CH11231. The Dark Cosmology Centre is funded by the Danish National Research Foundation.

[1] Planck Collaboration XV, arXiv:1303.5075.
[2] C. L. Bennett *et al.*, arXiv:1212.5225.
[3] J. Samsing, E. V. Linder, and T. L. Smith, Phys. Rev. D **86**, 123504 (2012).
[4] E. V. Linder and T. L. Smith, J. Cosmol. Astropart. Phys. 04 (2011) 001.
[5] E. V. Linder, Phys. Rev. D **82**, 063514 (2010).
[6] A. Lewis, A. Challinor, and A. Lasenby, Astrophys. J. **538**, 473 (2000); CAMB, http://camb.info.
[7] A. Lewis and S. Bridle, Phys. Rev. D **66**, 103511 (2002); COSMOMC, http://cosmologist.info/cosmomc.
[8] S. Das *et al.*, arXiv:1301.1037.
[9] K. T. Story *et al.*, arXiv:1210.7231; South Pole Telescope, http://pole.uchicago.edu/public/data/story12/index.html.
[10] W. Hu, Astrophys. J. **506**, 485 (1998).
[11] E. Calabrese, D. Huterer, E. V. Linder, A. Melchiorri, and L. Pagano, Phys. Rev. D **83**, 123504 (2011).
[12] M. Doran and G. Robbers, J. Cosmol. Astropart. Phys. 06 (2006) 026.
[13] Planck Collaboration XVI, arXiv:1303.5076.

[14] R. R. Caldwell and S. S. Gubser, Phys. Rev. D **87**, 063523 (2013).
[15] M. D. Niemack *et al.*, Proc. SPIE Int. Soc. Opt. Eng. **7741**, 77411S (2010).
[16] Z. Kermish *et al.*, Proc. SPIE Int. Soc. Opt. Eng. **8452**, 84521C (2012).
[17] J. E. Austermann *et al.*, Proc. SPIE Int. Soc. Opt. Eng. **8452**, 84520E (2012).